Ionisation injection LWFA with few-cycle sub-TW laser pulses*

D. Papp[1,†], E. Rácz[1,2], P. Antici[1,3,4], C. Kamperidis[1]

[1]: ELI-ALPS, ELI-HU Non-Profit Ltd., 6726 Szeged, Hungary, [2]: Óbuda University, 1034 Budapest, Hungary; [3]: INRS-EMPT, Varennes, Canada, [4]: INFN, 00187 Roma, Italy

[†]: corresponding author, daniel.papp@eli-alps.hu

The main mission of ELI-ALPS in Szeged, Hungary is to establish a user facility that provides attosecond secondary XUV sources and ultrafast high repetition-rate particle sources for external users, driven by unique few-cycle high repetition-rate laser systems [1]. This study investigates the expected Laser Wakefield Acceleration (LWFA) electron bunch parameters obtainable, as driven by the unique laser systems envisioned at ELI-ALPS.

Most studies on laser wakefield electron acceleration focus on high electron energies driven by >10s TW-class lasers, with the envisioned utilization as a LWFA betatron x-ray source [2], or as a GeV electron source for a free electron lasers [3]. For laser pulse energies in the mJ range optimal scaling requires both tight focusing and short, few-cycle laser pulses, but such lasers would also offer the possibility of high (kHz) repetition rates, like recent results from several research groups [4,5,6].

In the following work we discuss particle-in-cell (PIC) computational studies on LWFA based on the two high repetition-rate 1-6 TW laser systems to be available at the ELI-ALPS institute. The ALPS-HR2 laser system is an Er-fiber amplifier-based system with double hollow-core fiber post-compression to provide 1030 nm, 5 mJ, <6fs laser pulses at 100 kHz repetition rate. The ALPS SYLOS-1 system has already demonstrated 50 mJ, 9 fs laser pulses at 1 kHz [7], and it is expected to provide 30+ mJ, <6 fs laser pulses at 1 kHz repetition rate after final commissioning. The scaling of LWFA parameters, i.e. that the focal spot size should be comparable (and smaller) than the plasma wavelength, requires high electron densities ($>10^{19}$ cm^{-3}) at the expected focusing conditions. At these densities, intense self-evolution of the laser pulse, i.e. self-focusing and self-compression affect and determines the accelerated electron beam properties.

To facilitate electron injection, the ionization injection scheme [9] is used. The selected target gas was CO_2, where carbon enables low K-shell ionization energies, 372 eV for the 5th electron stripped from a neutral atom, according to the ADK theory [9], which corresponds to 3.8×10^{18}

* The ELI-ALPS project (GINOP-2.3.6-15-2015-00001) is supported by the European Union and co-financed by the European Regional Development Fund.

Wcm^{-2} laser intensity, when the barrier suppression ionisation mechanism is considered. CO_2 is used in our computational studies, as it relaxes significantly the safety considerations (non-flammable, non-toxic gas) compared to alternatives like CH_4 or CO. The laser intensity for the investigated cases was selected to match the ionization potential of K-shell Carbon electrons, i.e. to be around 5×10^{18} Wcm^{-2}.

Our simulations were conducted using the EPOCH particle-in-cell code in 2D geometry, with a moving window and the grid resolution along the propagation axis set at λ/33 μm. The atomic model assumes ground states only with sequential ionization, i.e. the outermost electrons is stripped always and accounts for multiphoton, field, and Barrier Suppression Ionization effects. The laser pulse was defined at the laser entrance boundary, with Gaussian spatial intensity distribution, with focusing provided by the appropriate phase distribution on the boundary, according to the paraxial approximation.

For simulations using the ALPS-HR2 driving laser parameters, the target was neutral gas with a longitudinal Gaussian density profile and a FWHM of 100 μm, i.e. representing the plasma generated from a sub-sonic gas jet. The investigated gases were H_2 - where ionization injection is not present - and CO_2. H_2 targets showed no electron injection at $n_e=4.2\times10^{19}$ cm^{-3}, and only marginal injection at higher densities and/or on the density downramp. Fig. 1. shows the electron density distribution and phase-space plots for a CO_2 target. Laser parameters were 5 mJ, 6 fs, 5 μm FWHM "vacuum" focal spot, focused at the half-maximum rising edge of the gas jet, achieving $I_{max} = 2.9\times10^{18}$ Wcm^{-2} and $a_0 = 1.5$ in vacuum, with a maximum electron density of $n_e = 4.2\times10^{19}$ cm^{-3}. The mean electron energy of the accelerated electron bunch is 19 MeV, the laser-to-electron efficiency of 0.81% and the inferred charge is 2 pC. Only electrons from Carbon V were injected into the bubble.

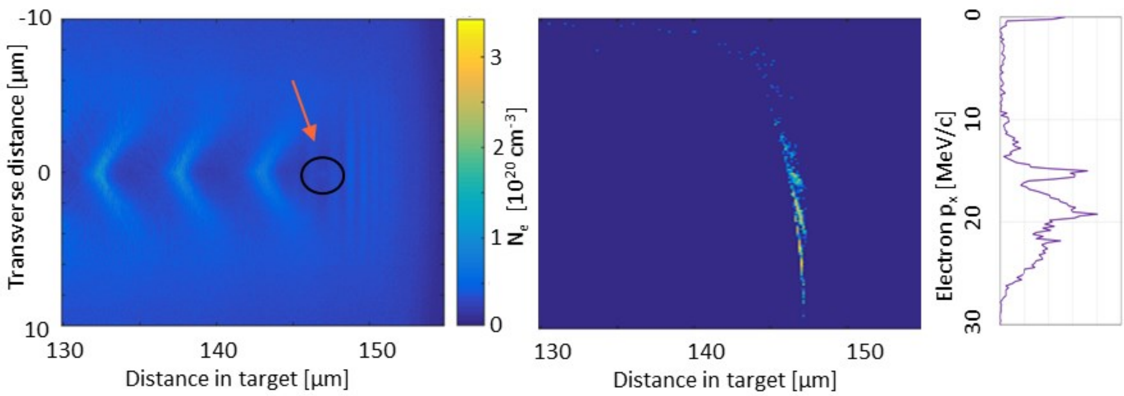

Figure 1. Total electron density (left), logarithmic x-p_x phase space plot (centre) for Carbon V electrons and the respective electron spectrum (right), achieved with the ALPS-HR2 laser system.

The envisioned applications of the 100 kHz electron beamline are ultrafast electron diffraction with quasi-monoenergetic, few-fs <5 MeV electron bunches, radiobiological experiments, betatron XUV source (up to 300 eV), and possibly Compton back-scattering x-ray source ($4\gamma^2\hbar\omega$ up to 10 keV).

In case of the 1kHz SYLOS laser, two separate scenarios were investigated. The first case uses the full beam energy for electron acceleration. The simulated target was a uniform density (flat density longitudinal profile) gas jet with 60 um wide linear ramp at the two edges, with a maximum electron density of $n_e = 2\times10^{19}$ Wcm^{-2} = $0.015n_c$ with the laser nominally focused at the start of the full-density gas jet. Laser parameters were 900 nm, 6 fs, 40 mJ with 10μm FWHM focal spot for a nominal vacuum $a_0 = 1.7$, which increased to $a_0 = 1.9$ from plasma self-focusing. This laser pulse generated extreme high bunch charge, 200 pC with a mean energy of 30 MeV (Fig. 2.).

The envisioned applications of the full-energy SYLOS-driven 1kHz electron beamline are radiobiological experiments, as a betatron soft x-ray source (~1 keV) and as a Compton back-scattering x-ray source (>15 keV).

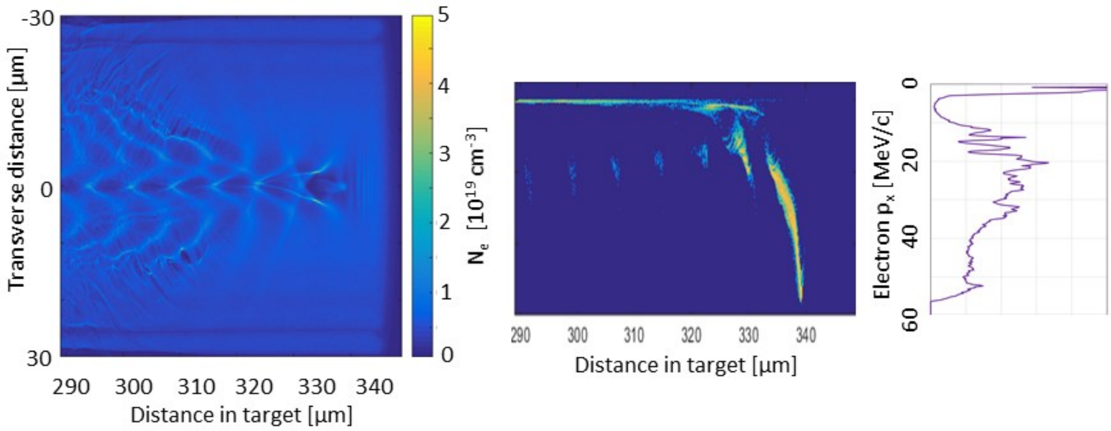

Figure 2. Total electron density (left), logarithmic x-p_x phase space plot for Carbon V electrons (centre) and the respective electron spectrum (right), achieved with the ALPS-SYLOS laser system.

The third investigated scenario assumes a LWFA-based inverse Compton back-scattering photon source with 50-50% energy split of the SYLOS laser. The simulated target was a gas jet of Gaussian density distribution and a FWHM of 200 um and a maximum electron density of 2×10^{19} cm^{-3}, with the laser nominally focused at the half-maximum density position on the rising edge. The 20 mJ, 6 fs laser pulse was focused to a 7.2 μm FWHM "vacuum" focal spot with an intensity of 4.6×10^{18} Wcm^{-2} and a0=1.66. The generated electron beam had 27 MeV average energy and 12 pC charge.

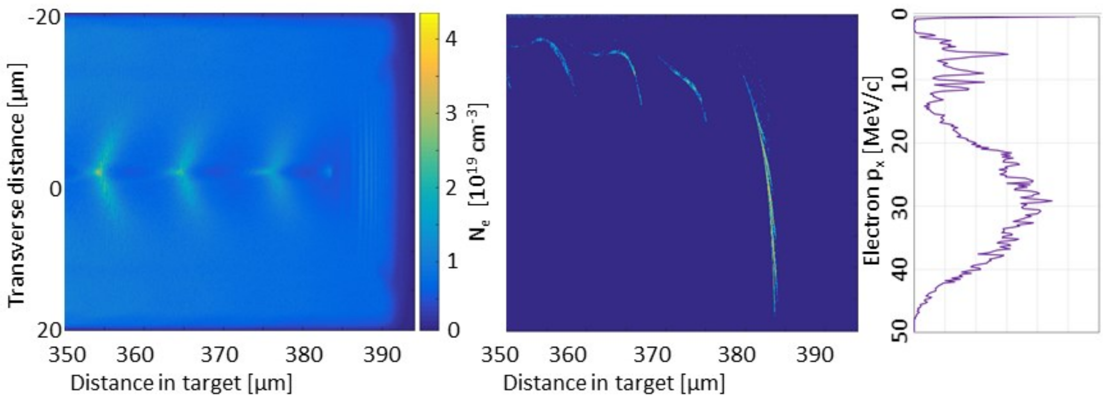

Figure 3. Total electron density (left), logarithmic x-p_x phase space plot for Carbon V electrons (centre) and the respective electron spectrum (right), achieved with the ALPS-SYLOS laser operating at half the expected laser energy.

Head-on collision of the electron bunch with the other half of the driving laser beam would produce inverse Compton-scattered electrons with x-ray energies upto $4\gamma^2\hbar\omega$~20-30 keV, an estimated x-ray output of 10^{10} photons/s and peak brilliance in the order of 10^{23} photons/mm^2/mrad^2/s (0.1% BW). This x-ray beam would be suitable for ultrafast x-ray probing with <10 fs temporal resolution.

The unique high laser systems available at ELI-ALPS are envisioned to produce relatively low - yet relativistic - energy electron beams at high repetition rates. Besides direct utilization, e.g. for ultrafast electron diffraction or radiobiological experiments, such LWFA-produced electron beams can also be used indirectly as a source of high brilliance few-fs XUV/x-rays, extending the available x-ray energy range at the facility for prospective experiments.

References

[1] http://eli-hu.hu/?q=en/01_What_is_ELI-ALPS%3F, retrieved 15.06.2017

[2] Esarey E. et al., PR E 65, 056505 (2002)

[3]https://www.eli-beams.eu/en/research/x-ray-sources/laser-undulator-x-ray-source-lux/, retrieved 23.06.2017

[4] Z-H. He et al., NJP 15, 053016 (2013)

[5] A.J. Goers et al., PRL 115, 194802 (2015)

[6] D. Guénot et al., Nat. Phot. 11, 293 (2017)

[7] R. Budriunas et al., Opt. Exp. **25**, 5797 (2017)

[8] M. Chen et al., PoP **19**, 033101 (2012)

[9] M. V. Ammonosov et al., Sov. Phys. JETP 64, 1191 (1986)